



Prediction of Reservoir Permeability from Petrography Characterisation

S. Baraka-Lokmane^{1,2,3}, I.G. Main¹, B.T. Ngwenya¹, S.C. Elphinstone¹

¹ School of GeoSciences, University of Edinburgh, UK

² Institute of Petroleum Engineering, Heriot-Watt University, Edinburgh, UK

³ School of Environment and Technology, University of Brighton, UK

**29th Course of the International School of Geophysiscs
Euro-Conference of "Rock Physics and Geomechanics" on Natural hazards: thermo-hydro-mechanical processes in rocks
(EMFCSC, Erice, Sicily, 25-30 September, 2007)**

Outline

- **Introduction**
- **Description of the rock material**
- **Fluid-rock interactions, regression results**
- **Conclusions**



Introduction

Reservoir quality, primarily determined by the **porosity** and **permeability** of the relevant formations, can be a function of many controls including:

- Nature of the constituent minerals and cement;
- Degree of rock cementation;
- Degree of sorting or equivalently the particle size of the grains;
- Pore-size distribution.

Reservoir engineers, petrophysicists and exploration geologists have tried to obtain quantitative relationships between 2-D petrographic properties and 3-D petrophysical properties.

McCreesh et al., 1991; Ehrlich et al., 1991; Gerard et al., 1992; Passas et al., 1996; Mowers and Budd, 1996; Anselmetti et al., 1998; Ioannidis et al., 1996

Purpose of this study

- 1- A detailed characterisation of three sandstone reservoir samples
 - Fife sandstone
 - Locharbriggs sandstone
 - Slick Rock Aeolian sandstone

- 2- Evaluation of the effect of mineralogy on permeability and prediction of reservoir permeability from petrography characterisation

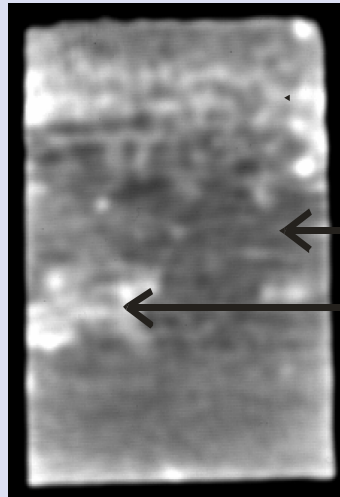
Description of Rock Material

- **X-ray Computer Tomography (CT-Scanner)**
- **Particle Size Analysis**
- **Petrography (thin sections analysis, using a point counting technique)**
- **Environmental Scanning Electron Microscopy (ESEM)**
- **X-Ray Diffraction (XRD) Analyses**
- **X-Ray Fluorescence (XRF) Analyses**
- **Petrophysical description - permeability and porosity**

X-ray Computer Tomography (CT-Scanner)

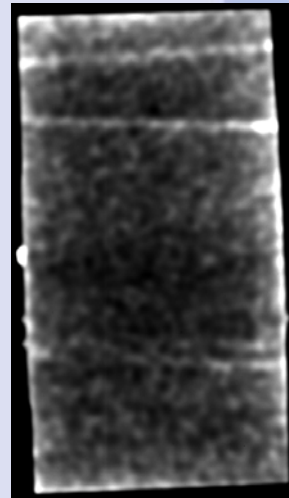
Method of measurement	Measured parameters	Comments on the advantages	Comments on the disadvantages
3-D X-ray Computer Tomography	<ul style="list-style-type: none"> • Rock heterogeneity • Presence of iron and calcite 	<ul style="list-style-type: none"> • Relatively rapid method of measurement • Not destructive method 	<ul style="list-style-type: none"> • Interpretation of the grey scale is challenging • Previous petrography analysis is necessary

X-ray Computer Tomography (CT-Scanner)



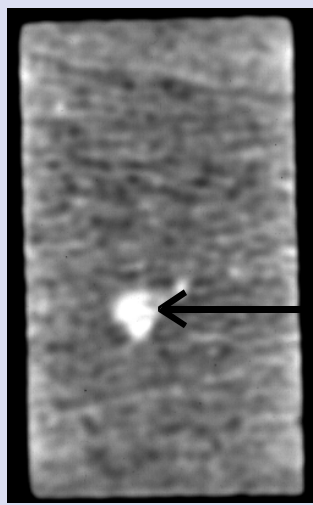
← Iron banding
← Calcite patch

Slick Rock Aeolian sandstone



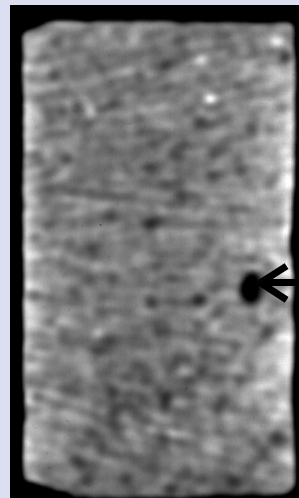
← Iron banding

Locharbriggs Sandstone



← Calcite

Fife sandstone

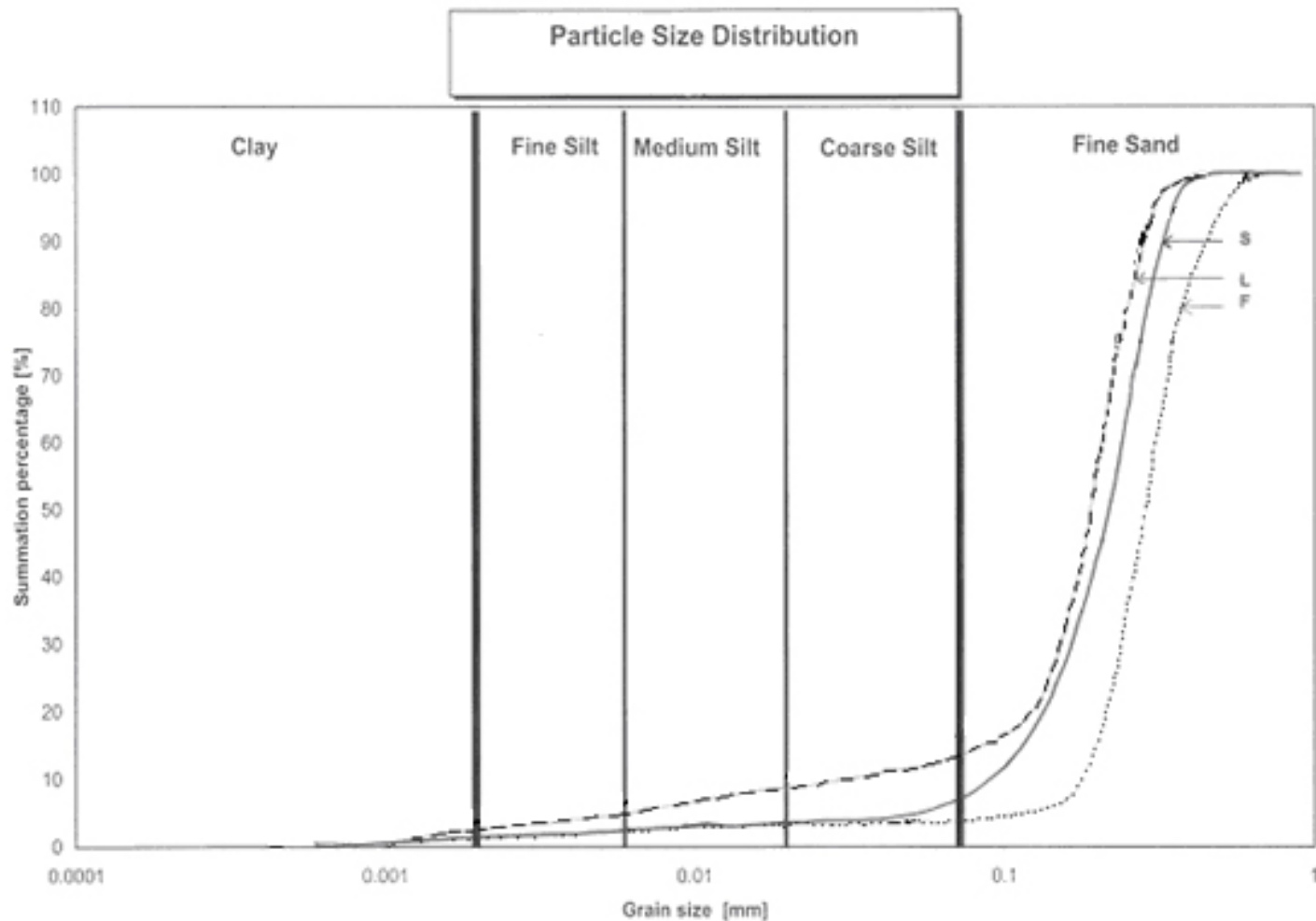


← Kaolinite

Fife sandstone



Particle Size Analysis





Particle Size Analysis

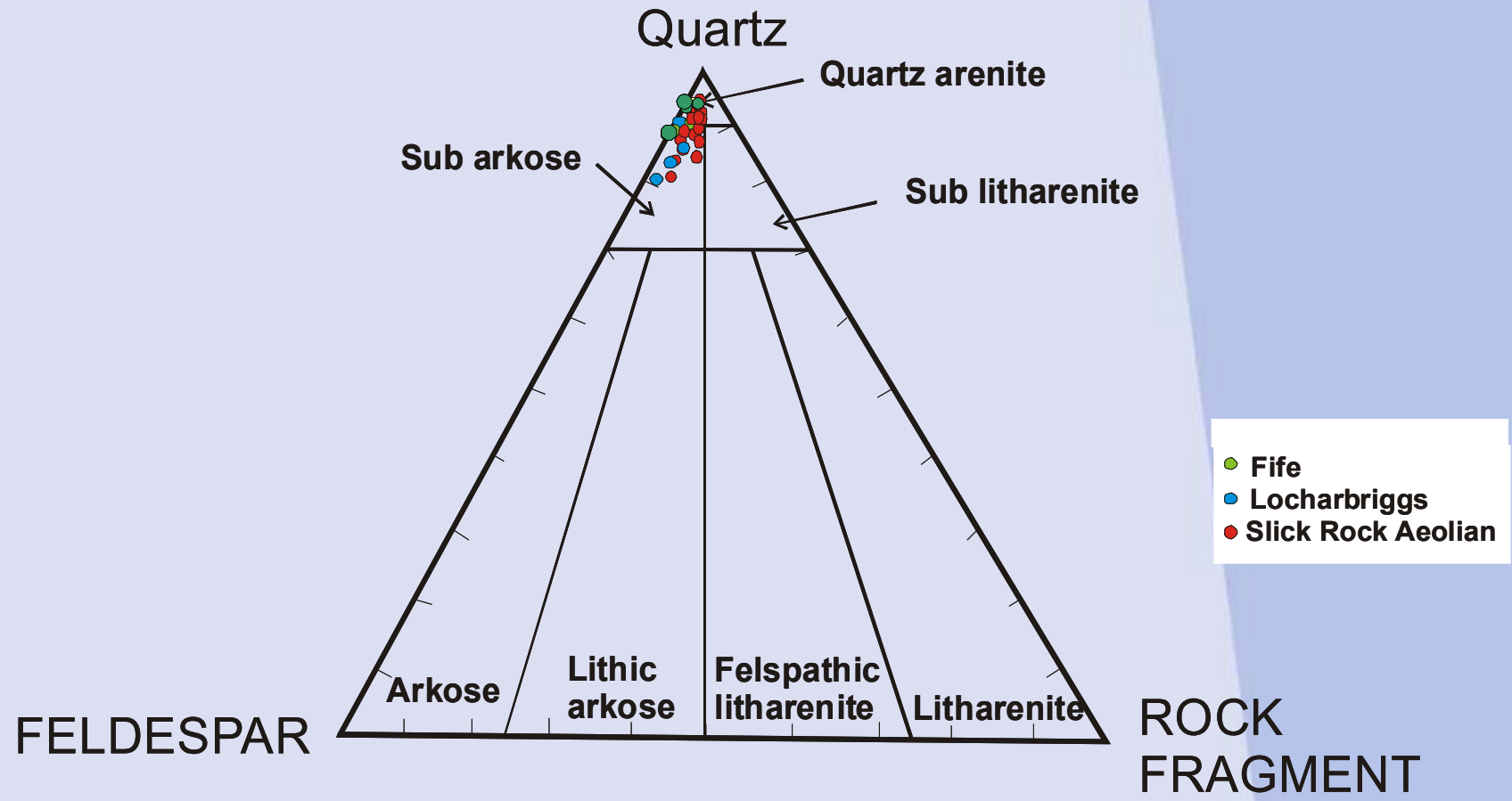
Method of measurement	Measured parameters	Comments on the advantages	Comments on the disadvantages
3-D Particle size	<ul style="list-style-type: none">• Rock heterogeneity• Mean grain size	<ul style="list-style-type: none">• useful to supplement porosity for empirical permeability estimation	<ul style="list-style-type: none">• Not always easy to obtain grains from a sandstone core



Petrography

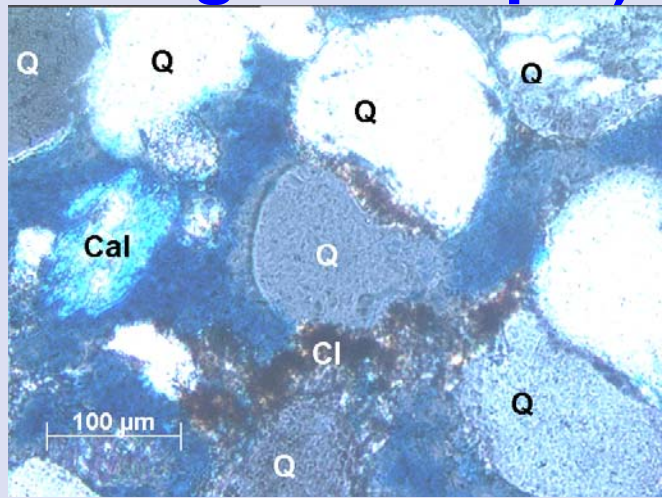
Method of measurement	Measured parameters	Comments on the advantages	Comments on the disadvantages
2-D Point counting using thin sections	<ul style="list-style-type: none"> Percentages of the different mineral constituents and porosity Identification of the dominant cement 	<ul style="list-style-type: none"> Structural analysis Identification of rare minerals 	<ul style="list-style-type: none"> Time consuming
3-D XRD	<ul style="list-style-type: none"> Mineralogy composition 	<ul style="list-style-type: none"> Quantitative analysis Independent method from point counting Identification of the different types of clays 	<ul style="list-style-type: none"> Minerals present with less than 1 % of the rock are not identified
3-D XRF	<ul style="list-style-type: none"> Chemical composition 	<ul style="list-style-type: none"> Quantitative analysis for most elements with concentrations as low as 1ppm 	<ul style="list-style-type: none"> time consuming

Petrography

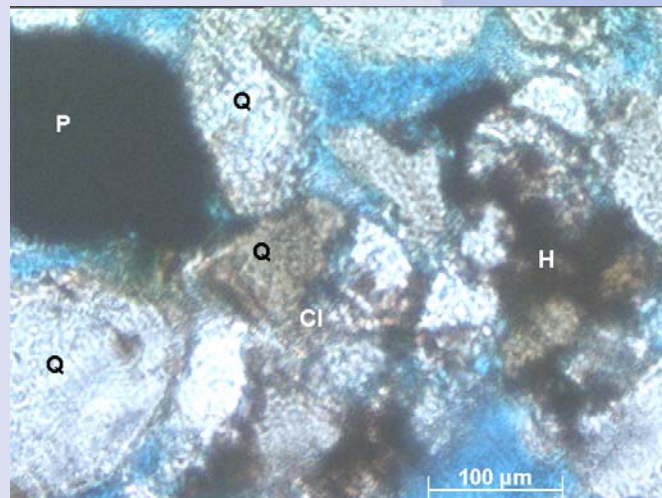


Composition of the three groups of samples shown in the Q-F-RF diagram of Folk (1974)

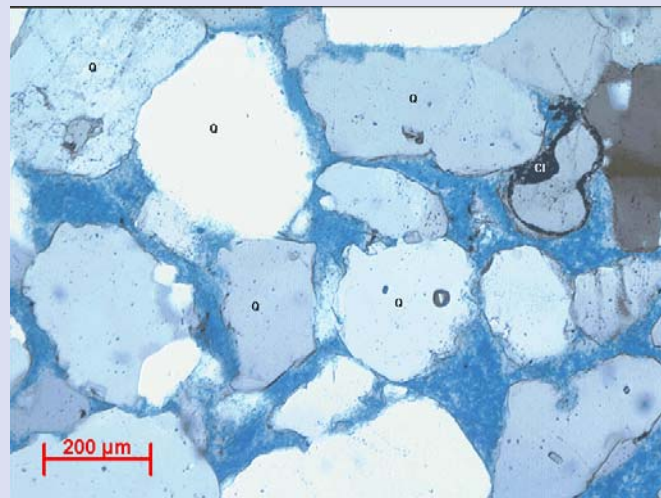
Petrography (thin sections analysis using point counting technique)



Slick Rock Aeolian sandstone



Locharbriggs Sandstone



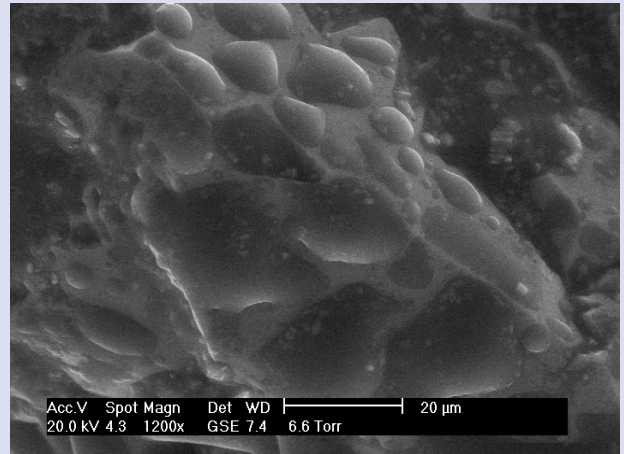
Fife sandstone

Environmental Scanning Electron Microscopy (ESEM) Measurements

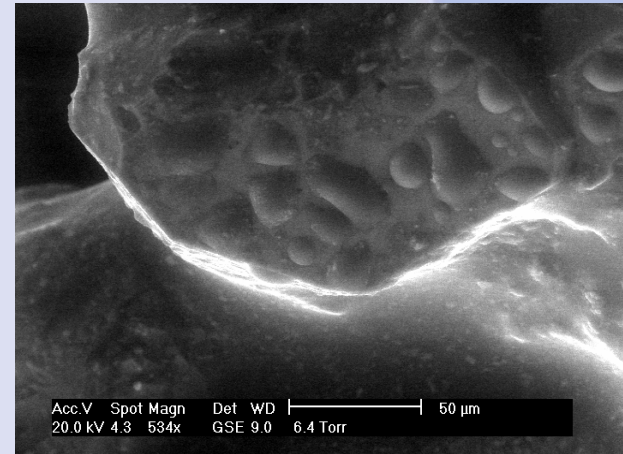
Method of measurement	Measured parameters	Comments on the advantages	Comments on the disadvantages
3-D ESEM/EDX	<ul style="list-style-type: none">•Wettability of the different minerals•Mineral identification	<ul style="list-style-type: none">•Relatively rapid method of measurement	<ul style="list-style-type: none">•Qualitative and not quantitative method of measurement



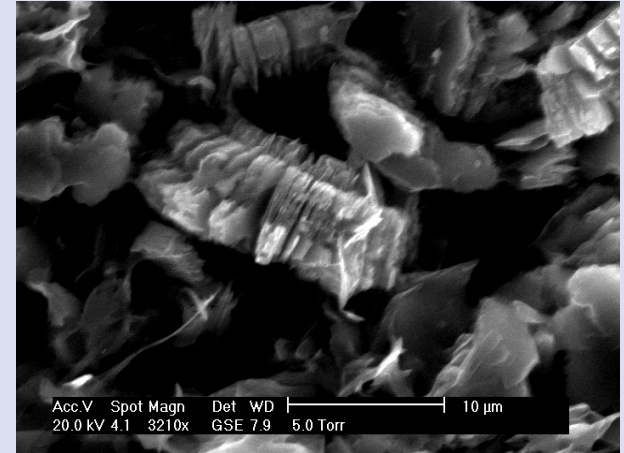
Environmental Scanning Electron Microscopy (ESEM) Measurements



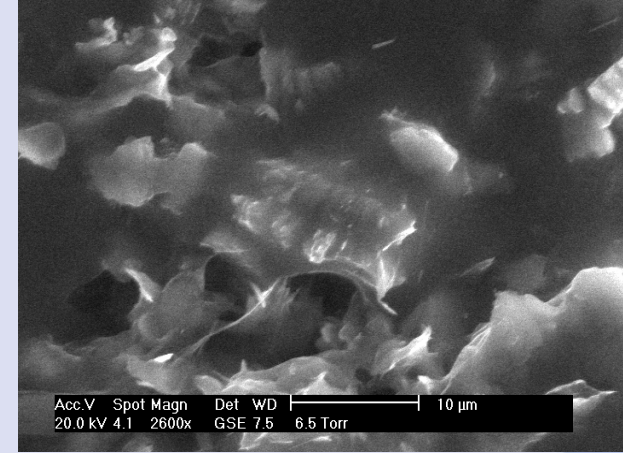
Water wet quartz



Water wet feldspar

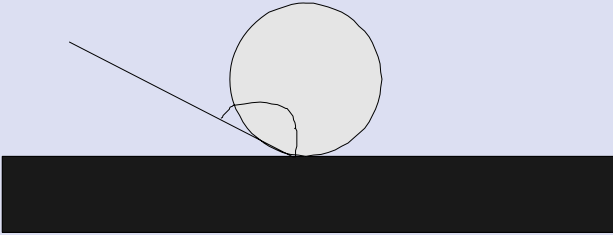


Cement containing kaolinite, smectite and illite

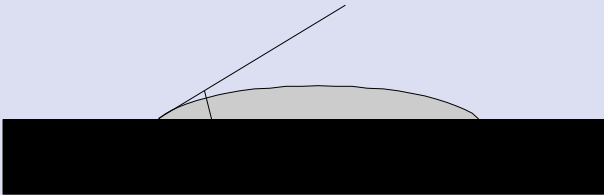


Very water wet clays

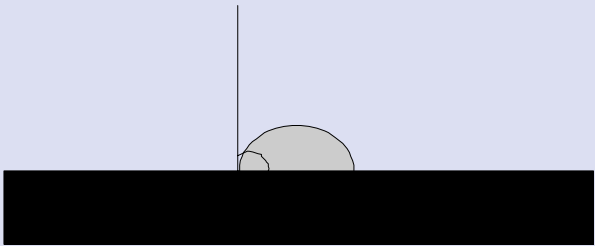
Environmental Scanning Electron Microscopy (ESEM) Measurements



Strongly oil wet condition



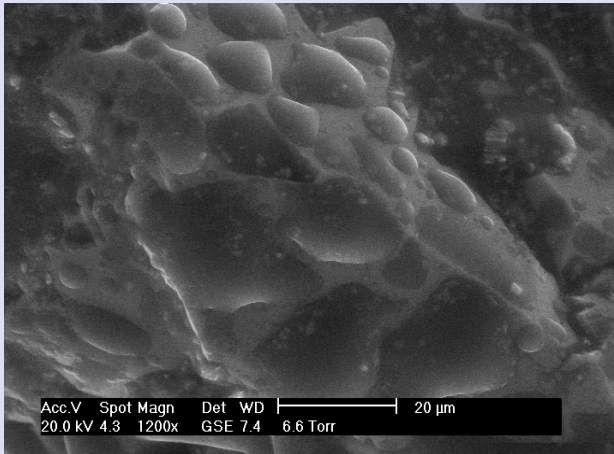
Strongly water wet condition



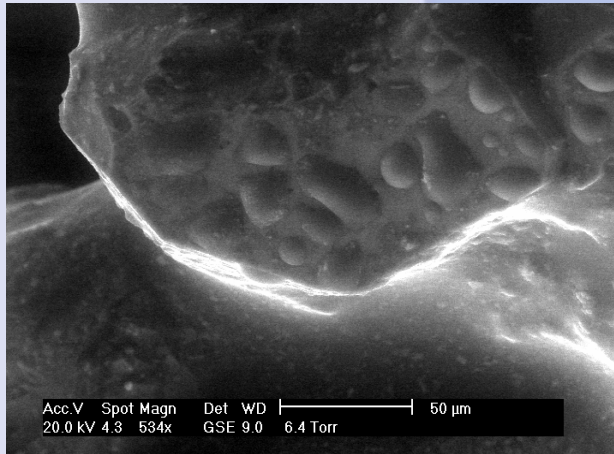
Intermediate in wetness condition

Schematic diagrams of three levels of wettability

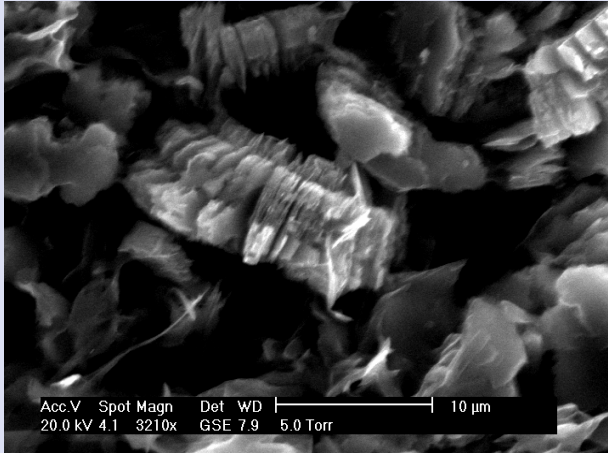
Environmental Scanning Electron Microscopy (ESEM) Measurements



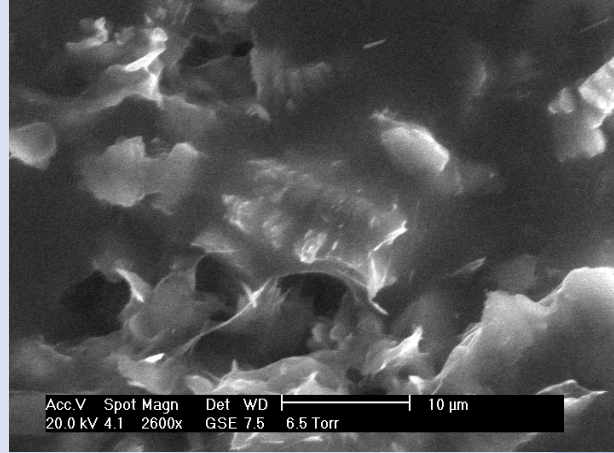
Water wet quartz



Water wet feldspar



Cement containing kaolinite, smectite and illite



Very water wet clays

Petrographical and petrophysical parameters of the 3 groups of samples

Sandstone	Locharbriggs	Slick Rock Aeolian	Fife
Brine permeability, k_i (mD)	706 ± 177	285 ± 71	1980 ± 388
Gas permeability, k_g (mD) (200 psi)	1424 ± 35	499 ± 49	1366 ± 63
k_g / k_i	2.1 ± 0.7	1.9 ± 0.6	0.7 ± 0.2
Porosity, Φ (%)	26.1 ± 0.1	22.3 ± 0.5	23 ± 3
Mean Grain size, MGS (μm)	199 ± 5	208 ± 28	348 ± 28
SiO₂ content (%)	92.9 ± 0.4	91.5 ± 0.4	97.5 ± 0.1
Cement content (%)	7 ± 2	10 ± 2	5 ± 1
Type of cement	illite, kaolinite, smectite, hematite	Calcite, illite hematite	kaolinite
Clays content (%)	6 ± 2	5.3 ± 0.9	5 ± 2
Type of clays	illite, kaolinite, smectite	illite	kaolinite



Fife sandstones

Fife sandstones present systematically different petrographical/petrophysical characteristics than Slick Rock Aeolian and Lochabriggs sandstones.

- Most homogeneous rock material; the main detrital components are represented by quartz;
- Largest percentage of SiO_2 content (97.5 %),
- Largest mean grain size (348 μm);
- Lowest percentage of cement (5 %).



These microstructural characterisations explain the highest values of permeability ($k \sim 1980 \text{ mD}$)

- Good agreements between gas and liquid permeability; the only clay minerals are kaolinite (5 %).

Slick Rock Aeolian and Locharbriggs sandstones

- Higher values of the ratio between gas and liquid permeability (kg/kl ~2).
- Illite (5.3%) for Slick Rock Aeolian sandstones
- Smectite, Illite and kaolonite (6 %) for Lochabriggs sandstones.

The swelling clays are responsible for the reduction of the liquid permeability.

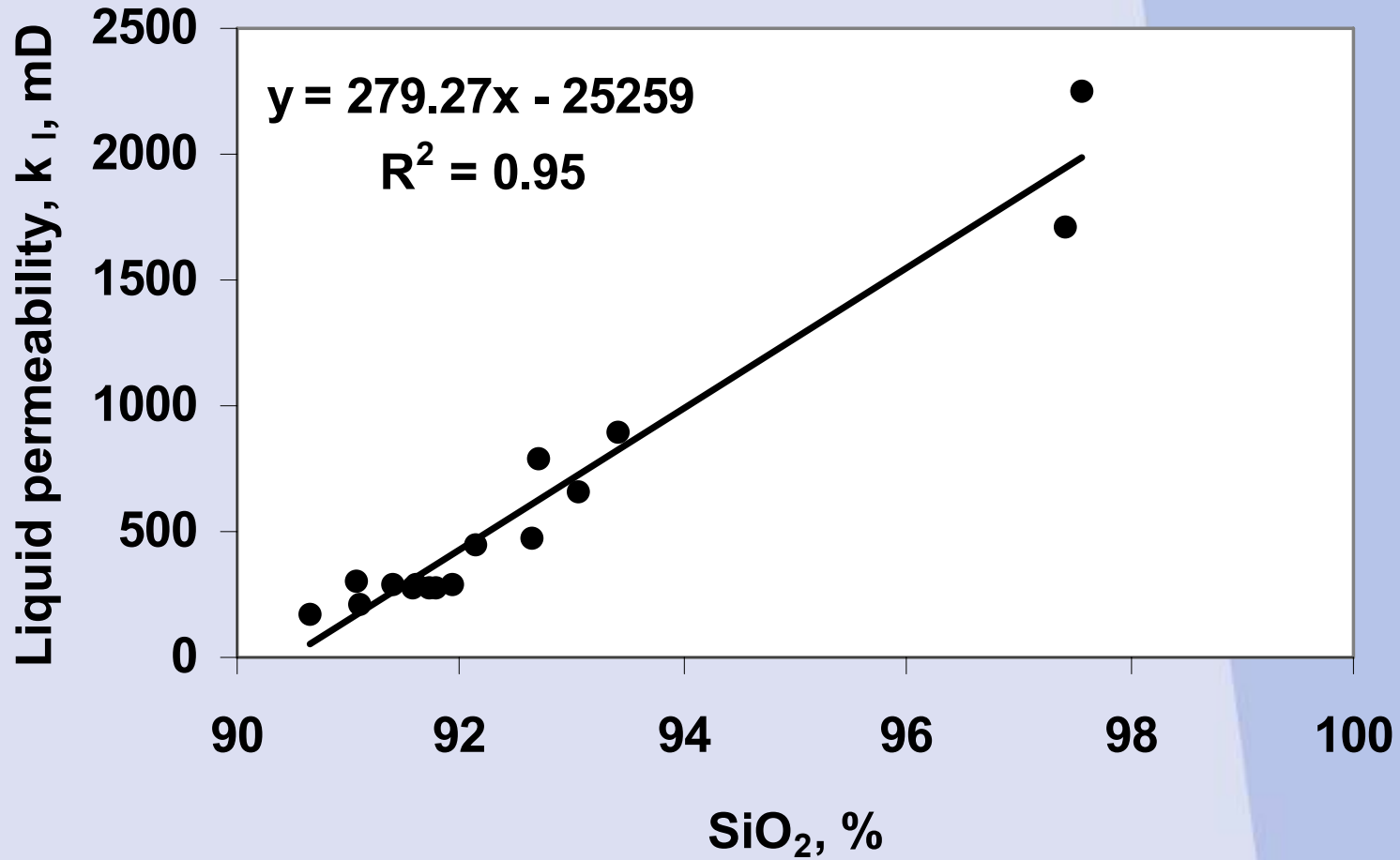
- **Smectite** tends to swell when exposed to brine. It is very hydrophilic due to its “mobile” structure.
- **Illite** is a mineral that reacts with brine to a limited extent.
- **Kaolinite** is not prone to swelling with changes in water content. Kaolinite, having a stable, “rigid” structure (due to the strong book bonds) reacts with water to a minimum extent

Fluid-Rock Interactions

Liquid permeability is correlated to 1 to 5 petrographical / petrophysical parameters such as

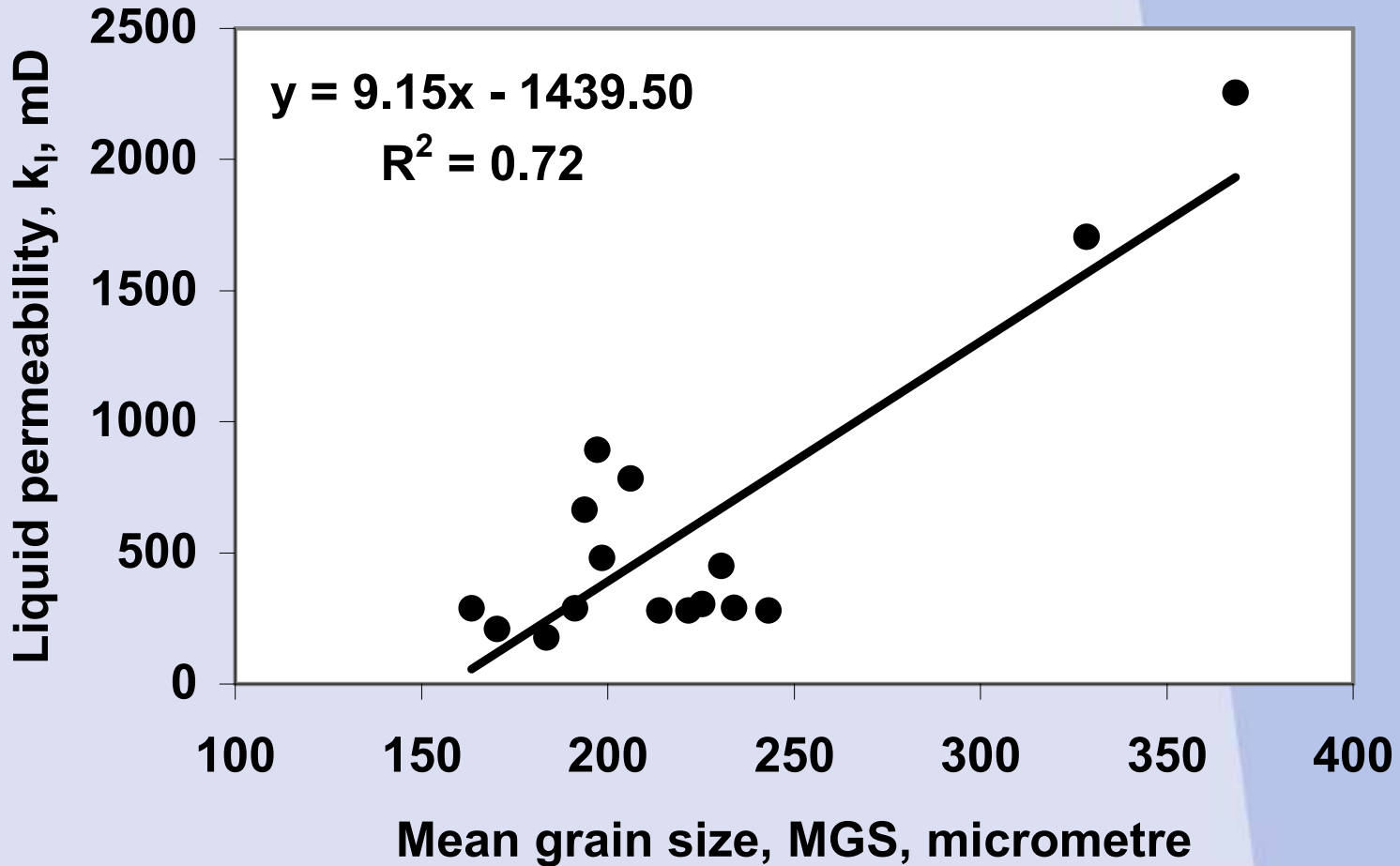
- SiO_2 ,
- Clay,
- Cement
- Porosity
- Mean grain size (MGS)

Fluid-Rock Interactions



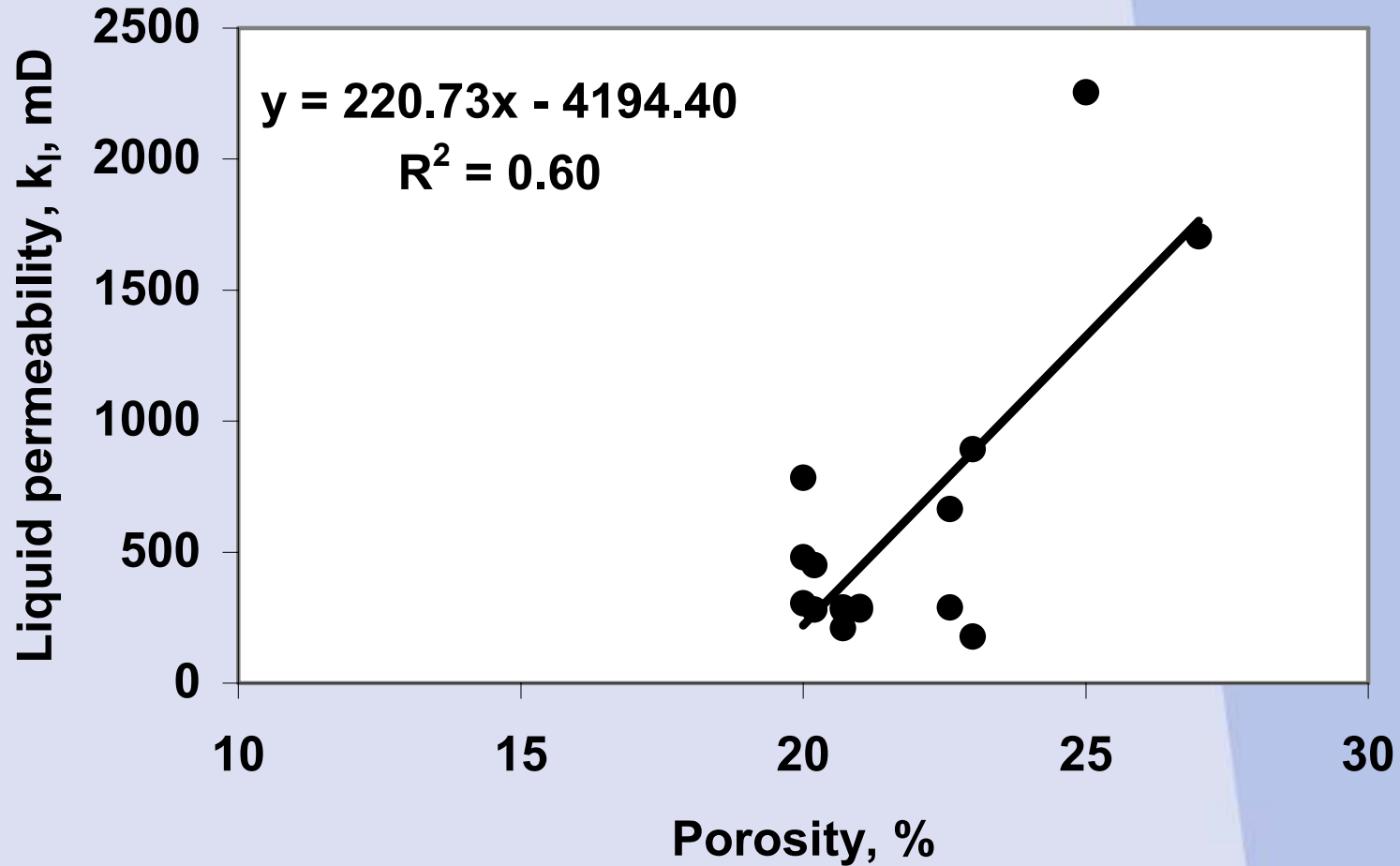
Cross-plots for k_l versus percentage of SiO_2

Fluid-Rock Interactions



Cross-plots for k_l versus mean grain size (MGS)

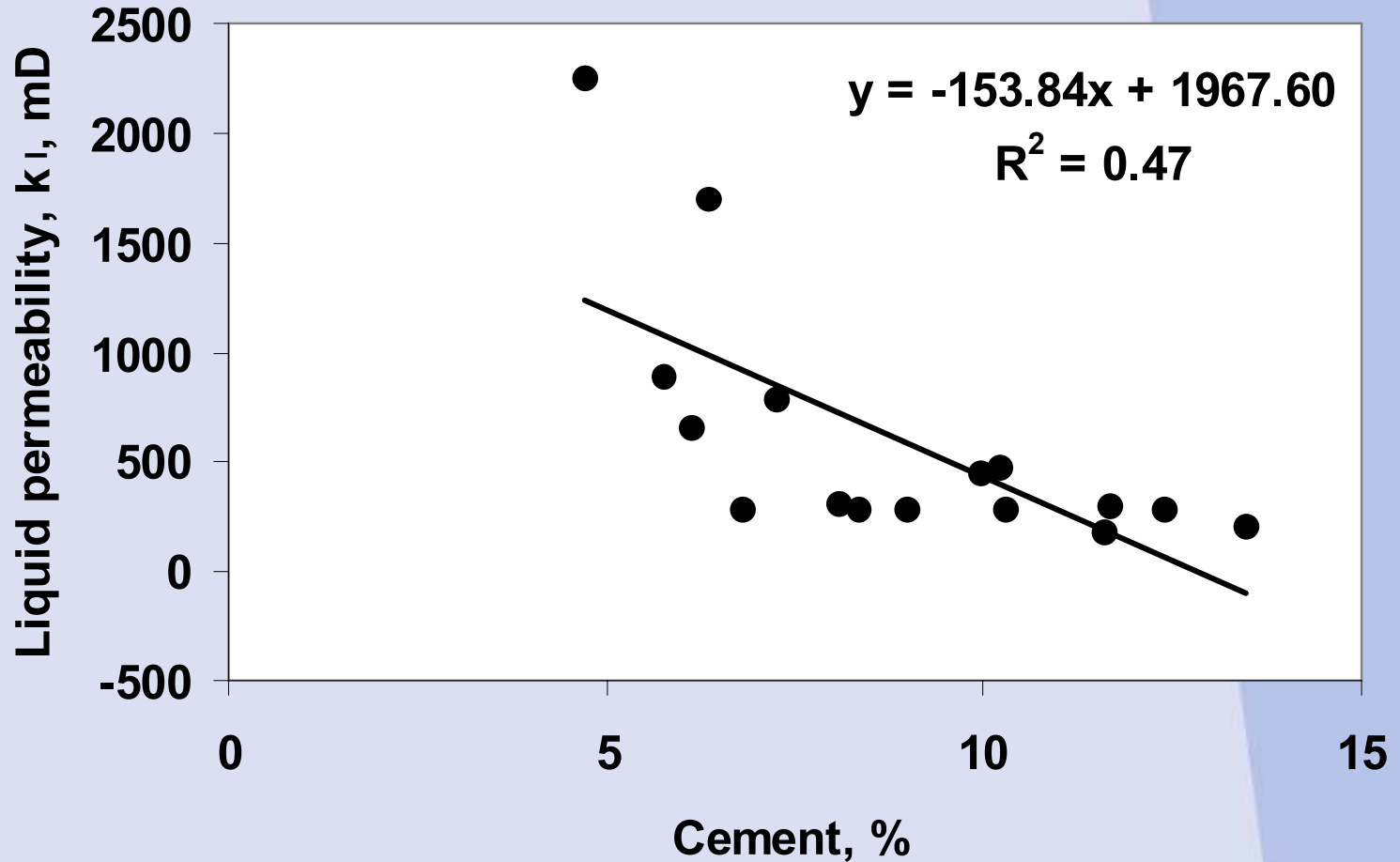
Fluid-Rock Interactions



Cross-plots for k_l versus percentage of porosity



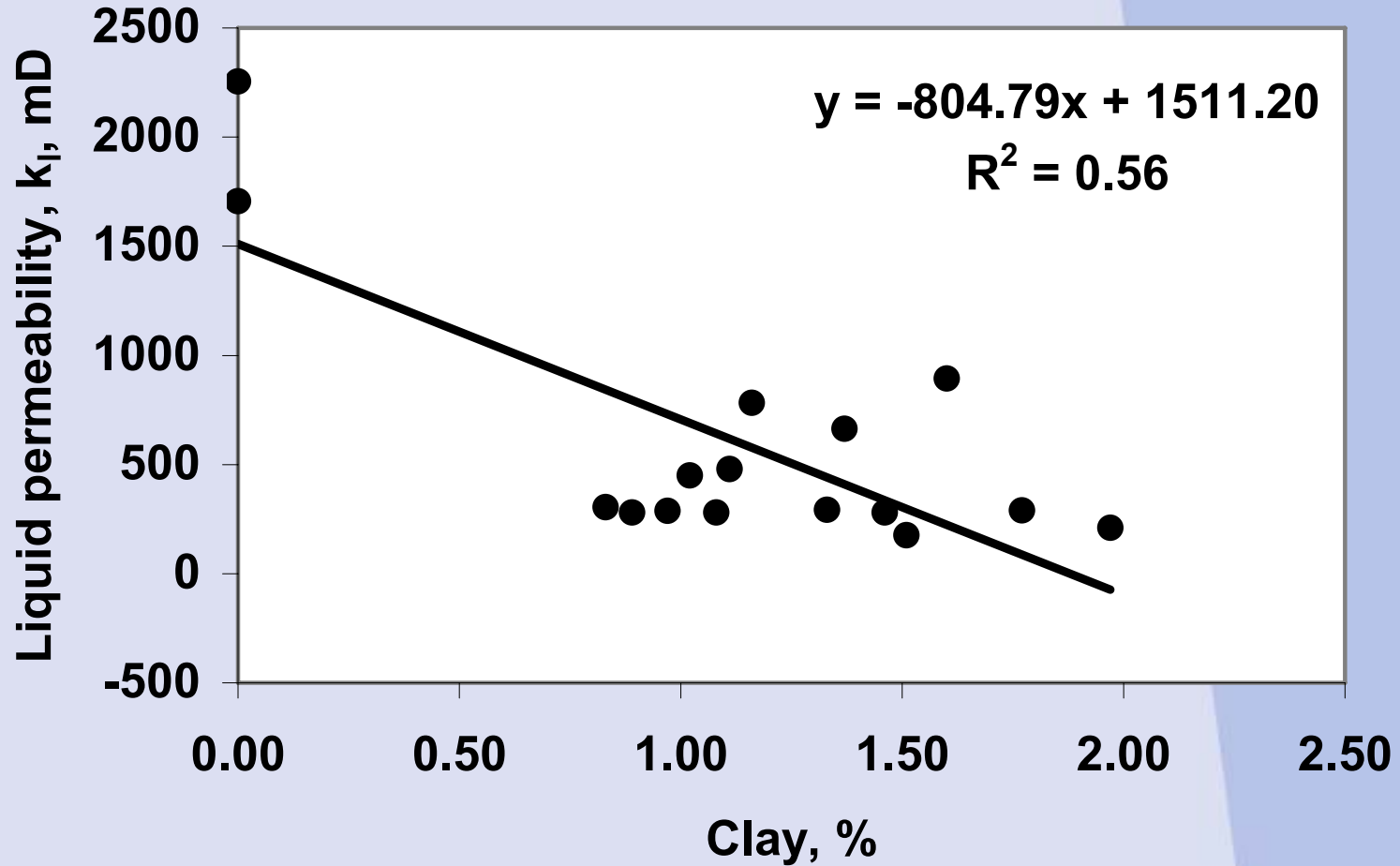
Fluid-Rock Interactions



Cross-plots for k_l versus percentage of cement



Fluid-Rock Interactions



Cross-plots for k_i versus percentage of clay



Regression results

Multi-variate regressions were performed using 2 to 5 variables of petrographic elements

Calculated parameters:

- Correlation coefficient (R^2),
- Standard deviations (S.D.)
- Akaike's Information Criterion (AIC)

Akaike information criterion (AIC) H. Akaike (1973)

$$AIC3 = \left(-\left[\frac{n}{2}\right] * LnML\right) - p$$

where

n is the number of data points in the regression

p is the number of independently adjusted parameters within the model

ML is the maximum likelihood method

Ln is the natural log

$$ML = \sum (obs - pred)^2$$



Regression results

Physical Sciences



Variables: petrographic elements	Least squares fit	R ²	S.D.	AIC
SiO ₂	a. $k_1 = 279.27\% \text{ SiO}_2 - 25259.20$	0.95	132.44	-100.30
MGS	b. $k_1 = 9.15\mu\text{m MGS} - 1439.50$	0.72	319.35	-114.38
Φ	c. $k_1 = 220.73\% \Phi - 4194.40$	0.60	392.63	-117.68
Cement	d. $k_1 = -153.84\% \text{ Cement} + 1967.60$	0.47	439.83	-119.49
Clay	e. $k_1 = -804.79\% \text{ Clay} + 1511.20$	0.56	402.37	-118.07
SiO ₂ , MGS	f. $k_1 = 254.11\% \text{ SiO}_2 + 1.13 \mu\text{m MGS} - 23181.2$	0.95	132.68	-99.74
SiO ₂ , Clay	g. $k_1 = 283.78\% \text{ SiO}_2 + 21.88\% \text{ Clay} - 25701$	0.94	137.20	-101.68
SiO ₂ , Φ	h. $k_1 = 285.41\% \text{ SiO}_2 - 7.86\% \Phi - 25656.60$	0.94	137.04	-100.25
SiO ₂ , Cement	i. $k_1 = 265.82\% \text{ SiO}_2 - 15.84\% \text{ Cement} - 23872.60$	0.95	133.35	-99.81
MGS, Φ	j. $k_1 = 6.61\mu\text{m MGS} + 113.16\% \Phi - 3331.46$	0.79	267.65	-110.96
MGS, Cement	k. $k_1 = 7.27\mu\text{m MGS} - 77.39\% \text{ Cement} - 331.71$	0.78	273.31	-111.29
SiO ₂ , MGS, Clay	l. $k_1 = 259.75\% \text{ SiO}_2 + 2.20\mu\text{m MGS} + 142.96\% \text{ Clay} - 24102.9$	0.95	131.51	-98.96
SiO ₂ , MGS, Cement	m. $k_1 = 235.27\% \text{ SiO}_2 + 1.28\mu\text{m MGS} - 18.25\% \text{ Cement} - 21308.2$	0.95	132.31	-99.05
SiO ₂ , Cement, Clay	n. $k_1 = 266.92\% \text{ SiO}_2 - 15.68\% \text{ Cement} + 4.70\% \text{ Clay} - 23981.40$	0.94	138.78	-99.81
SiO ₂ , Clay, Φ	o. $k_1 = 294.77\% \text{ SiO}_2 + 34.14\% \text{ Clay} - 10.85\% \Phi - 26496.90$	0.94	142.09	-100.19
SiO ₂ , MGS, Φ	p. $k_1 = 257.14\% \text{ SiO}_2 + 1.10 \mu\text{m MGS} - 3.20\% \Phi - 23386.4$	0.94	138.03	-99.73
MGS, Cement, Φ	q. $k_1 = 5.69\mu\text{m MGS} - 59.35\% \text{ Cement} + 89.68\% \Phi - 2089.31$	0.83	238.75	-108.49
MGS, Clays, Φ	r. $k_1 = 5.73\mu\text{m MGS} - 97.57\% \text{ Clay} + 114.65\% \Phi - 3056.58$	0.78	277.06	-110.88
SiO ₂ , MGS, Clay, Φ	s. $k_1 = 272.01\% \text{ SiO}_2 + 2.22\mu\text{m MGS} + 158.13\% \text{ Clay} - 12.34\% \Phi - 24992.4$	0.95	136.31	-98.83
SiO ₂ , MGS, Cement, Φ	t. $k_1 = 236.19\% \text{ SiO}_2 + 1.27\mu\text{m MGS} - 18.20\% \text{ Cement} - 0.92\% \Phi - 21371.8$	0.94	138.18	-99.05
SiO ₂ , MGS, Cement, Clay	u. $k_1 = 242.86\% \text{ SiO}_2 + 2.20\mu\text{m MGS} - 15.71\% \text{ Cement} + 125.82\% \text{ Clay} - 22379.9$	0.95	132.77	-124.63
SiO ₂ , Cement, Clay, Φ	v. $k_1 = 275.45\% \text{ SiO}_2 - 15.09\% \text{ Cement} + 14.15\% \text{ Clay} - 7.79\% \Phi - 24617.7$	0.94	144.56	-99.77
SiO ₂ , MGS, Cement, Clay, Φ	w. $k_1 = 252.86\% \text{ SiO}_2 + 2.21\mu\text{m MGS} - 15.00\% \text{ Cement} + 138.02\% \text{ Clay} - 9.30\% \Phi - 23127.4$	0.94	138.61	-98.34

Results

Best Model

$$k_1 = 272.01\% \text{ SiO}_2 + 2.22\mu\text{m MGS} + 158.13\% \text{ Clay} - 12.34\% \Phi - 24992.4$$

$$R^2 = 0.95$$

$$S.D. = 136.31$$

$$AIC = -98.83$$



Conclusions

This study shows that the permeability of sandstone cores can be predicted from the measurement of the percentages of silica (SiO_2), which can be performed with the help of XRF analyses using only 50 g of material from rock sample.

The results obtained in this study have useful application in the estimation of reservoir permeability where samples are not available for experimental testing.

Conclusions

The results of the different methods used were found to be consistent with each other, but the combination of a variety of methods has allowed a more complete characterisation of the rock samples than each method used on its own.

This study has shown that rock heterogeneity at the sub-cm scale may have a significant effect on reservoir petrophysical characterisation.

X-ray Computer Tomography (CT-Scanner)

The total radiological density depends on both the mineralogical and chemical composition of the rock and the porosity. The radiological density is expressed in Hounsfield modified units (H.M.U.).

- Very dark grey: quartz and feldspar, they have a physical density varying between 2.55 and 2.76 g/cm³. The quartz and feldspar have a low radiological density varying between -120 H.M.U. and -160 H.M.U.
- Dark grey: kaolinite, it has a low physical density (2.60 g/cm³).
- Light grey: muscovite and illite, they have a medium physical density (2.80 g/cm³) and therefore a medium radiological density due to the presence in their chemical formula of potassium.
- Light grey: potassium feldspars (microcline) have a medium radiological density (-50 H.M.U.) and a physical density (2.59 g/cm³).
- White: calcite is a very attenuating mineral; it has a physical density of 2.71 g/cm³ and a high radiological density (241 H.M.U.). Calcite, though only slightly denser (2.71 g/cm³) than quartz and potassium feldspar, is substantially more attenuating, owing to the presence of calcium.
- White: hematite has a physical density higher than the other minerals (5.26 g/cm³) and therefore a high radiological density due to the presence in its chemical formula of iron.

In sandstone cores, calcite and ferromagnesian minerals would likely be registered as an anomaly in X-ray scan.